

# C2G2: Controllable Co-speech Gesture Generation with Latent Diffusion Model

Longbin Ji<sup>1,2</sup>, Pengfei Wei<sup>2</sup>, Yi Ren<sup>2</sup>, Jinglin Liu<sup>2</sup>, Chen Zhang<sup>2</sup>, Xiang Yin<sup>2</sup>

<sup>1</sup>Xi'an Jiaotong Liverpool University  
<sup>2</sup>Bytedance

longbin.ji19@student.xjtlu.edu.cn, {wei.pengfei, ren.yi, liu.jinglin, zhangchen.990620, yinxiang.stephen}@bytedance.com

## Abstract

Co-speech gesture generation is crucial for automatic digital avatar animation. However, existing methods suffer from issues such as unstable training and temporal inconsistency, particularly in generating high-fidelity and comprehensive gestures. Additionally, these methods lack effective control over speaker identity and temporal editing of the generated gestures. Focusing on capturing temporal latent information and applying practical controlling, we propose a *Controllable Co-speech Gesture Generation* framework, named **C2G2**. Specifically, we propose a two-stage temporal dependency enhancement strategy motivated by latent diffusion models. We further introduce two key features to C2G2, namely a speaker-specific decoder to generate speaker-related real-length skeletons and a repainting strategy for flexible gesture generation/editing. Extensive experiments on benchmark gesture datasets verify the effectiveness of our proposed C2G2 compared with several state-of-the-art baselines. The link of the project demo page can be found at [https://c2g2-gesture.github.io/c2\\_gesture](https://c2g2-gesture.github.io/c2_gesture).

## Introduction

Gestures that accompany speech play an essential role in human communication, providing significant support for expressing personality, emotions, and motivations of speakers. Existing studies (Goldin-Meadow 2005; Goldin-Meadow and McNeill 1999; Nyatsanga et al. 2023) have shed light on the functions of gestures including the ability to convey motions with more communicative information and prevent excessive redundancy through mimetic expression. As a result, the generation of appropriate co-speech gesture behaviors using AI models is one of the crucial branches in achieving Artificial General Intelligence (AGI).

Existing co-speech gesture generation methods can be broadly divided into two categories, namely rule-based and data-driven approaches. Early works (Cassell et al. 1994; Huang and Mutlu 2012) predominantly fall under the rule-based category, where gestures are selected from a pre-built gesture pool based on specifically designed heuristics. However, these methods often lack diversity in the generated gestures due to their heavy reliance on predefined rules. In contrast, recent research has shifted the focus towards data-driven approaches, aiming to learn the association between speech and corresponding gestures from the wild data using deep learning-based models (Alexanderson et al. 2020; Ao

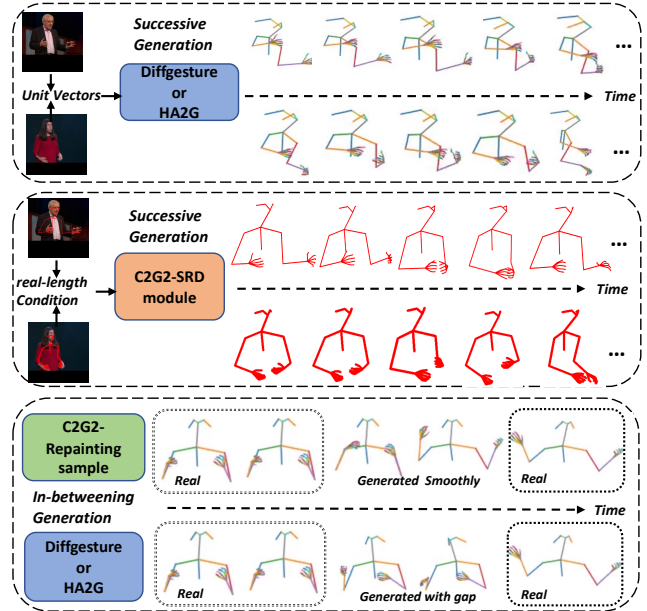


Figure 1: Controlling features of C2G2: speaker-related real-length gesture generation and flexible editing. The upper figure shows the *successive* and *unit-vectored* gesture generation of existing methods; the intermediate figure shows the *successive* and *speaker-related real-length* gesture generation by C2G2; the lower figure shows the *in-betweening* gesture generation by C2G2.

et al. 2022). Among them, GAN-based models (Yoon et al. 2020; Liu et al. 2022) have attracted increasing attention as they can produce realistic and reliable gestures by using adversarial loss.

However, GAN-based approaches may encounter the issues of mode collapse and unstable training, leading to the unsatisfactory performance. A recent work (Zhu et al. 2023) proposes a *DiffGesture* framework that uses the diffusion model (Ho, Jain, and Abbeel 2020) for co-speech gesture generation. By reformulating the multi-frame gesture clip as the diffusion latent space, it successfully generates clip of gestures in a non-autoregressive manner. However, *DiffGesture* simply uses a transformer block to capture the long-term temporal dependency and only leaves the potential tem-

poral inconsistency to be alleviated in the sampling process, which degenerates the generation quality of comprehensive finger movements.

Recently, latent diffusion model (Rombach et al. 2022) is proposed for high-quality generation tasks. By discovering a prior latent space, the model can remove redundant information and preserve the semantic variation for the diffusion process. This motivates us to enhance the temporal coherence in co-speech gesture generation using a two-stage procedure. In the first stage, we propose to train a temporal-aware Vector Quantized Variational AutoEncoder (VQ-VAE) augmented with a cross-frame attention module, which allows the model to capture temporal dependencies among frames before the quantization step. This helps to learn latent temporal-aware codes for the skeleton data, which are more expressive and temporally coherent. In the second stage, we use a diffusion process to enhance the temporal dependency between gesture and audio data, which is similar as (Zhu et al. 2023) but with a crucial difference. Instead of performing the diffusion process directly in the data space, we conduct the diffusion in the latent temporal-aware space obtained from the first stage. This allows to better model and preserve the temporal relationships between gestures and audios, leading to more synchronized and coherent co-speech gesture generation.

Moreover, we note that existing methods generate co-speech gestures with some limitations. On one hand, the generated results are usually skeletons represented by unit direction vectors (Liu et al. 2022; Zhu et al. 2023) or joints from SMPL-X with consistent shape (Ao, Zhang, and Liu 2023), that generally overlook the speaker information. On the other hand, the generation is successively done conditioned on short previous frames, which may result in uncontrollable or unreasonable gestures in a long run. These limitations highly jeopardize the downstream tasks like human-body rendering or animation synthesis.

To this end, we propose a *Controllable Co-speech Gesture Generation* framework with latent diffusion, called **C2G2**. The C2G2 framework overcomes the limitations of previous methods by introducing two key features. The first key feature is the inclusion of a speaker-conditioned decoder. By incorporating the speaker’s identity or characteristics as conditioning information, C2G2 enables the generation of personalized gestures that align with the specific speaker’s style and mannerisms. The second key feature is the introduction of a repainting strategy during the sampling process. This strategy provides flexibility and control over the gesture generation by allowing users to generate and edit gestures in any time intervals. With this feature, we can generate both successive and in-betweening gestures. Combining these two features with latent diffusion, the C2G2 framework promises to achieve more smoothed and controllable co-speech gesture generation. To sum up, this paper makes the following contributions:

- Based on the latent diffusion model, we propose a two-stage co-speech gesture generation model with two-stage temporal dependency enhancement. Extensive experiments on benchmark datasets show the effectiveness of our proposed C2G2 compared with current state-of-the-

art methods.

- We develop a speaker-specific control module, that is capable of generating speaker’s real length skeletons instead of unit vectors.
- We propose a gesture editing control module through a repainting strategy to allow arbitrary gesture editing in the long-sequence generation.

## Related work

Generating synthesized gesture for corresponding text/audio has been an important research interest in fields of computer visual graphics and multimedia. Earlier methods mainly applies rule-based searching (Cassell et al. 1994; Marsella et al. 2013) or statistic models (Yang, Yang, and Hodgins 2020) to select the appropriate gesture in a pre-defined motion pool for a given speech input. With the development of deep learning models, more studies start to use data-driven approaches to associate speech with the corresponding gestures. Some works apply CNN (Kucherenko et al. 2019), GRU or LSTM (Ishi et al. 2018), Transformer (Bhattacharya et al. 2021; Ahuja and Morency 2019) to generate gesture conditioned on texts (Bhattacharya et al. 2021; Ao, Zhang, and Liu 2023), audio (Li et al. 2021a) or mixed input (Ahuja et al. 2020a).

Recent works (Ginosar et al. 2019b; Ferstl, Neff, and McDonnell 2020; Ahuja et al. 2020b,a) focus on GAN based model due to its high-fidelity generation quality. Being a contributive work, (Liu et al. 2022) applies a hierarchical pose generator HA2G for part-aware progressive generation, and achieves natural and high-quality gestures. Motivated by the fact that different body parts have different levels of correlation with speech signals, Talkshow (Yi et al. 2023) leverages part-aware expert model with discrete representation to generate head, pose and hand, separately. Following the idea of taming transformer (Esser, Rombach, and Ommer 2020), Lu et al. (Lu, Yoon, and Feng 2023) propose to learn discrete tokens for a chunk of gestures and then auto-aggressively generate these tokens using a transformer block. With the same idea of (Lu, Yoon, and Feng 2023), (Ye et al. 2023) further considers the text condition in the second stage. Moreover, there are also methods focusing on emotive controlling by introducing style block as extra condition in diffusion or transformer generation procedure (Ahuja et al. 2020b; Qi et al. 2023; Ao, Zhang, and Liu 2023).

Very recently, Zhu et al. (Zhu et al. 2023) propose a *Diffgesture* framework that uses a diffusion model (Ho, Jain, and Abbeel 2020) to directly generate sequential input skeletons given audio input, capable of generating high-quality gestures with detailed finger movements. The generation results outperform previous methods. However, although *Diffgesture* applies a transformer audio-gesture noise predictor, the generated motion still has temporal inconsistency and uncontrollable collapse. Beyond this, it still suffers from the two limitations as elaborated in the Introduction. To overcome these issues, we propose a C2G2 framework with a two-level temporal dependency enhancement and allow speaker-related controlling and flexible editing within the latent diffusion generation.

## Method

Our objective is to produce co-speech gestures that exhibit high quality, temporal smoothness, and controllability, while maintaining coherence with the input audios. To do so, we present a novel *Controllable Co-speech Gesture Generation* framework, empowered by latent diffusion, called **C2G2**. The overall architecture of C2G2 consists of two modules: temporal-aware VQ-VAE and gesture latent diffusion model. The former is designed to capture the temporal coherence of gesture sequences through a sequence of discrete latent codes. On the other hand, the latter employs a diffusion process to generate a diverse range of latent embedding sequences conditioned on the input audios, encoding the temporal dependency of multi-modal inputs. Moreover, we introduce two enhancements, a speaker-related decoder (SRD) that is conditioned on a random reference frame and a repainting strategy that empowers both successive and in-betweening gesture generation. The SRD decoder directly generates skeletons tied to the speaker, deviating from the conventional approach of generating unit vectors. The repainting strategy facilitates flexible editing of generated gestures, enabling finer control over the generated animations. The details of each module are presented as follows.

### Preliminary

We start with the problem formulation of co-speech gesture generation. The inputs include the upper-body gesture joint sequences and the corresponding audios. Precisely, to obtain accurate gesture movements, state-of-the-art pose estimators Openpose (Cao et al. 2017) and Expose (Choutas et al. 2020b) are used to extract  $T$ -frames joint sequences  $\mathbf{x} = \{\mathbf{x}_1, \mathbf{x}_2, \dots, \mathbf{x}_T\}$ , as well as the matched audio sequence  $\mathbf{a} = \{\mathbf{a}_1, \mathbf{a}_2, \dots, \mathbf{a}_T\}$ . Following (Yoon et al. 2020; Liu et al. 2022; Zhu et al. 2023), a normalization step is applied to eliminate the speaker identity, resulting in the unit direction vector  $\mathbf{x}_i = \{\mathbf{d}_{i_1}, \dots, \mathbf{d}_{i_{J-1}}\}$  with  $J$  as the number of total joints and  $\mathbf{d}_{i_j}$  representing the direction vector between the  $j$ -th and the  $(j+1)$ -th joint of the  $i$ -th frame. The reason of conducting such a normalization is for the stable training of the following models as diversified-length skeletons may easily cause model collapse. However, to achieve the speaker-related real-length gesture generation, we also preserve real-length direction vectors  $\mathbf{s}_i = \{\mathbf{s}_{i_1}, \dots, \mathbf{s}_{i_{J-1}}\}$ . In C2G2, a temporal-aware VQ-VAE is first trained to reconstruct the unit direction vectors  $\mathbf{x}_i$ s, and then a speaker-related decoder is trained to generate the real-length direction vectors  $\mathbf{s}_i$ s conditioned on arbitrary reference frame  $\mathbf{s}_r$ . The reverse process of the latent diffusion model learns to synthesize the latent embedding  $\{\mathbf{z}_1, \mathbf{z}_2, \dots, \mathbf{z}_T\}$  given the audio input  $\mathbf{a}$  and the latent embedding of  $N$  previous frames,  $\{\mathbf{z}_1, \mathbf{z}_2, \dots, \mathbf{z}_N\}$ , which is obtained from VQ-VAE.

### Temporal-aware VQ-VAE

We first introduce a temporal-aware VQ-VAE to learn the latent codes for input joints sequences. Given a gesture sequence  $\mathbf{x} = [\mathbf{x}_1, \mathbf{x}_2, \dots, \mathbf{x}_T]$ , VQ-VAE aims to reconstruct the gesture sequence through a temporal-aware encoder-decoder structure and a quantized codebook  $C$  containing  $k$

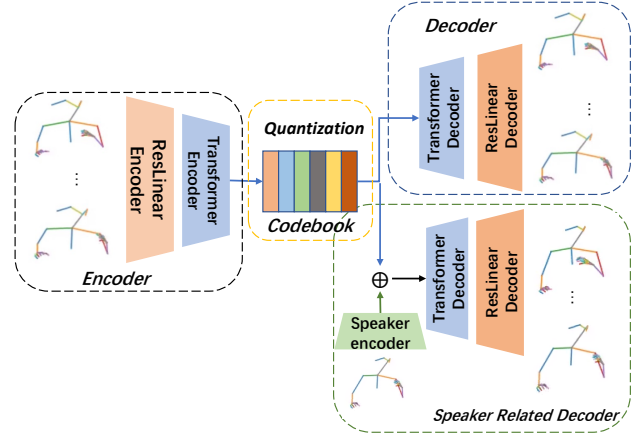


Figure 2: The structure of the temporal-aware VQVAE.

codes. The fundamental architecture of the proposed VQ-VAE is a symmetric encoder-decoder structure as shown in the top half of Figure 6. To better quantize comprehensive sequence containing the fingers of both hands, the encoder  $E$  consists of two stacking modules: a content extractor that is composed with linear based ResNet blocks, and a context encoder that uses cross-frame attention modules with positional encoding to capture the temporal coherence embedded in the long-term sequence. It maps the input sequence to a latent embedding  $\mathbf{z} = [\mathbf{z}_1, \mathbf{z}_2, \dots, \mathbf{z}_T]$ . Afterwards, the quantizer  $Q$  finds the corresponding latent codes  $\mathbf{c} = [\mathbf{c}_1, \mathbf{c}_2, \dots, \mathbf{c}_T]$  from the codebook  $C$  by optimizing:

$$\mathbf{c}_i = \operatorname{argmin} \|\mathbf{z}_i - \mathbf{c}_i\|_2, \mathbf{c}_i \in C.$$

The matched latent codes are then feed into the decoder  $D$  to reconstruct the sequence. The overall learning objective contains two components: a reconstruction loss and a commitment loss, where the former effectively measures the generating quality and the latter encloses the distance between the codes and latent features.

**EMA Quantization Strategy** In the training, the quantizer may easily stuck into the codebook collapse issue due to the high dimensionality of the training data. To provide smooth codebook updating, exponential moving average (EMA) and codebook reset strategies are implemented to avoid possible collapse due to inactive codes (Zhang et al. 2023; Razavi, Van den Oord, and Vinyals 2019). Reset strategy replaces the inactive codes according to the output of the encoder. EMA smooths the upgrading of the codebook  $C$  by  $C_T = \mu C_{T-1} + (1 - \mu)C_T$ . We provide an ablation study for the quantizer structure in experimental studies.

**Speaker Related Decoder** The above structure works on the input sequence represented by unit direction vectors and thus overlooks the speaker identity information. To generate the speaker specific real-length gestures, we further propose a speaker-conditioned decoder  $D_s$  as shown in the bottom half of Figure 6. The main difference of  $D_s$  from  $D$  is on an extra speaker encoder. The speaker encoder, which is composed of MLP and convolutional layers, is used to extract the speaker identity information from an arbitrary prompting

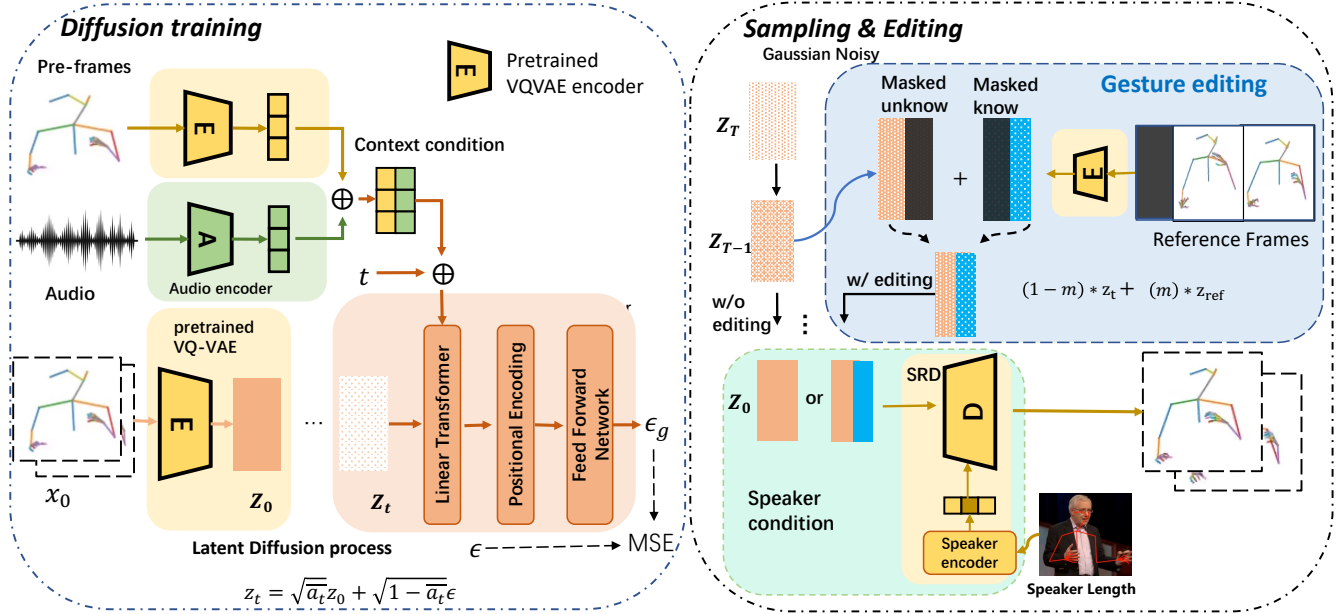


Figure 3: The framework overview of C2G2. Given input skeleton sequence  $\mathbf{x}$ , a pre-trained VQ-VAE will be used to generate latent embedding  $\mathbf{z}_0$  in latent space representation. Then diffusion forward process will turn  $\mathbf{z}_0$  into  $\mathbf{z}_T$ . A transformer based noise predictor will be applied for reverse denoising procedure. A speaker related real-length decoder will enable speaker controlling by extracting length information from given speaker condition. During sampling, we propose a repainting sampling strategy for in-betweening generation.

frame  $s_r$ , and then concatenate it with the latent codes. Note that, to keep the previously learned quantized code space stable, the encoder  $E$  and the quantizer  $Q$  are frozen and only the speaker related decoder is trained on the real-length direction vectors.

### Latent Diffusion Model

To generate reliable and diverse gestures, we leverage latent diffusion model (LDM) for the latent embedding generation. The core idea of LDM is to gradually denoise the Gaussian noise (Dhariwal and Nichol 2021; Rombach et al. 2022; Huang et al. 2023). Formally, LDM defines bi-directional process: forward diffusion and reverse denoising.

In forward process, LDM assumes that the process of adding noise based on the variance schedule  $\beta_t$  follows the Markov chain (Rombach et al. 2022). Through variances schedule  $\beta_t$ , the input distribution is finally corrupted into a pure noise with the Gaussian distribution  $\mathcal{N}(\mathbf{z}_T; \mathbf{0}, \mathbf{I})$ . Based on the independent property of the noise schedule, given  $\bar{\alpha}_t = \prod_{s=1}^t (1 - \beta_s)$ , the forward process can be summarized into one step:

$$q(\mathbf{z}_t|\mathbf{z}_0) := \mathcal{N}(\mathbf{z}_t; \sqrt{\bar{\alpha}_t}\mathbf{z}_0, (1 - \bar{\alpha}_t)\mathbf{I}). \quad (1)$$

Reverse denoising, i.e., the generation process, models the conditional distribution of  $p_\theta(\mathbf{z}_{t-1}|\mathbf{z}_t, \Phi)$  through the predicted noise given the context  $\Phi$ . For the co-gesture generation task,  $\Phi$  is the combination of the latent embedding of previous  $N$  frames  $\{\mathbf{z}_1, \dots, \mathbf{z}_N\}$  and audio features  $\mathbf{a}$ .

$$p_\theta(\mathbf{z}_{t-1}|\mathbf{z}_t, \Phi) = \mathcal{N}(\mathbf{z}_{t-1}; \mu_\theta(\mathbf{z}_t, t, \Phi), \beta_t\mathbf{I}). \quad (2)$$

To further boost the temporal dependency across frames for the latent sequence, we leverage the context measuring capacity of transformer for sequence modelling. Contextual information including previous  $N$  frames and audio features are concatenated together with  $\mathbf{z}_t$  in the feature channel. A self-attention module is then applied to discover the long-term temporal dependency. In the sampling process, to achieve the trade-off between diversity and temporal consistency, we adopt the *thresholding*, *smoothing sampling* and *classifier-free guidance* tricks as used in (Zhu et al. 2023).

### In-betweening Gesture Generation

To achieve flexible co-speech gesture generation, we further consider the in-betweening generation scenario where the first  $N$  frames and the last  $M$  frames are given and the aim is to generate intermediate temporally smooth gestures. Existing methods only support for successive generation, and generally fail in this scenario.

In our C2G2, we propose a repainting strategy, motivated by (Lugmayr et al. 2022), to generate the intermediate sequences by sampling from a mask region of conditional input. For every reverse step, with the given gesture frames  $\mathbf{Z}_c = [\mathbf{Z}_f, \mathbf{Z}_l]$ , where  $\mathbf{Z}_f$  and  $\mathbf{Z}_l$  represent the latent embedding of the first and the last frames, respectively, we can sample  $\mathbf{z}_{t-1}$  using:

$$\mathbf{z}_{t-1}^{known} \sim \mathcal{N}(\sqrt{\bar{\alpha}_t}\mathbf{Z}_c, (1 - \bar{\alpha}_t)\mathbf{I}), \quad (3)$$

$$\mathbf{z}_{t-1}^{unknown} \sim \mathcal{N}(\mu_\theta(\mathbf{z}_t, t, \Phi), \beta_t\mathbf{I}), \quad (4)$$

$$\mathbf{z}_{t-1} = \mathbf{m} \cdot \mathbf{z}_{t-1}^{known} + (1 - \mathbf{m}) \cdot \mathbf{z}_{t-1}^{unknown}, \quad (5)$$

Methods	TED Gesture			TED Expressive		
	FGD ↓	BC ↑	Diversity ↑	FGD ↓	BC ↑	Diversity ↑
Ground Truth	0.000	0.698	108.525	0.000	0.703	178.827
VQ-VAE Reconstruction	0.109	0.636	107.450	0.402	0.703	179.743
Att-S2S (Yoon et al. 2019)	18.154	0.196	82.776	54.920	0.152	122.693
S2G (Ginosar et al. 2019a)	19.254	0.668	93.802	54.650	0.679	142.489
L2P (Ahuja and Morency 2019)	22.083	0.200	90.138	64.555	0.130	120.627
TriM (Yoon et al. 2020)	3.729	0.667	101.247	12.613	0.563	154.088
HA2G (Liu et al. 2022)	3.072	<b>0.672</b>	104.322	5.306	0.641	173.899
DiffGesutre (Zhu et al. 2023)	1.506	<b>0.699</b>	<b>106.722</b>	2.600	<b>0.718</b>	182.757
C2G2 (Ours)	<b>1.035</b>	0.647	<b>106.991</b>	<b>1.168</b>	0.708	<b>182.824</b>
C2G2- <i>rl</i> (Ours)	<b>0.652</b>	0.615	73.066	<b>1.095</b>	<b>0.716</b>	<b>192.716</b>

Table 1: The quantitative results on TED Gesture and TED expressive datasets. We compare our C2G2 against ground-truth target and recent state-of-the-art methods. Herein, *rl* is to mark the model with SRD to generate speaker conditioned real-length gestures. The winner of each metric is highlighted using bold, and the runner-up is highlighted using bold and italic.

where  $\mathbf{m}$  is a mask indicating the unknown and known areas. Note that this repainting strategy does not require the re-training of LDM, and only works in the sampling process. With this strategy, we allow in-betweening editing in a long-term gesture sequence generation. Especially during autoregressive generation process, considering the randomness brought by probabilistic modelling, such flexible editing can be used in any step to interpolate expected gestures like hand shaking for reliable controlling.

## Experimental Studies

In this section, we first compare C2G2 with several state-of-the-art co-speech gesture generation baselines, and then conduct comprehensive property analyses of C2G2.

### Datasets Description

**Ted Gesture** (Yoon et al. 2020) is a large-scale English-based dataset for co-speech gesture generation, composed of 1766 TED videos from various topics and different narrators. The 3D gesture joints of human upper body as well as the corresponding audio sequence are available. Following the data pre-processing of previous works (Zhu et al. 2023; Razavi, Van den Oord, and Vinyals 2019; Yoon et al. 2020), pose frames are sampled in 15 FPS A clip segmentation consists of 34 video frames with 10-frame as the stride. Both unit direction and real-length vectors are extracted for gesture representation.

**Ted Expressive** (Liu et al. 2022) is a recent English-based dataset for co-speech gesture generation. Different from Ted Gesture dataset that only contains body skeletons, Ted Expressive extracts 30 finger joints using ExPose (Choutas et al. 2020a) for each frame to harvest diverse and detailed gesture representation. Based on SMPL-X (Pavlakos et al. 2019) 3D human parameterized model, ExPose joints can be directly turned into shape related human poses for further rendering. Same as in Ted Gesutre, both unit direction and real-length vectors are preserved for the following gesture generation.

## Experimental Settings

**Comparing baselines.** We compare our C2G2 with: 1) **Attention Seq2Seq** (Att-S2S) (Yoon et al. 2019) that leverages attention mechanisms for temporal gesture generation given texts; 2) **Speech2Gesture** (S2G) (Ginosar et al. 2019a) that uses cross-model translation model taken audio as input for movement generation; 3) **Language2Pose** (L2P) (Ahuja and Morency 2019) that learns a joint embedding space for language and pose clip; 4) **Trimodel** (TriM) (Yoon et al. 2020) that combines information from text, audio and speaker identity; 5) **HA2G** (Liu et al. 2022) that applies hierarchical audio-gesture generator across multiple level semantic granularity; and 6) **Diffgesture** (Zhu et al. 2023) that uses diffusion based model with sampling stabilizer for diverse gesture generation.

**Implementation Details.** For all the experiments, we sample 34 frames for generation and 4 precondition reference frames following (Yoon et al. 2020). The number of joints is 10 and 43 for TED Gesture and TED expressive, respectively. For the temporal-aware VQVAE, the content extractor is composed of 8 layers of linear Residual blocks, and the temporal extractor is a  $R$ -layer transformer encoder containing positional embedding, self attention and feed-forward Network where  $R = 4$  in the encoder and  $R = 2$  in the decoder. The quantizer is based on EMAReset as mentioned in Section 3.1 where the updating rate  $\mu = 0.9$ . For SRD, the speaker reference encoder is composed of 3 layers of Residual blocks that outputs a 64-dimensional embedding vector. For the latent codebook with  $N_C$   $d_C$ -dimensional codes,  $N_C = 1024$ ,  $d_C = 64$  for TED Gesture and  $N_C = 1024$ ,  $d_C = 128$  for TED Expressive. For the audio encoder, we use the structure in (Yoon et al. 2020) to extract information from raw audios. A conditional frame encoder that is used to process the given 4 frames share the weights of VQ-VAE encoder.

For the latent diffusion module, the denoising step is 500 and the variance schedule is linearly increasing from  $1e - 4$  to 0.02. The transformer module is a 8-layers transformer



encoder with self-attention and feed-forward Network. The hidden dimension of the transformer is 256 for both TED Gesture and TED Expressive. We use Adam as the optimizer with the learning rate  $5e-4$  for TED Gesture and  $3e-4$  for TED Expressive. The training is done on a single NVIDIA A100 GPU. For the VQ-VAE training, it takes  $\sim 6$  hours for TED Gesture and  $\sim 14$  hours on TED Expressive. For the diffusion module training, it takes  $\sim 8$  hours on TED Gesture and  $\sim 20$  hours on TED Expressive.

**Evaluation Metrics.** We adopt three widely used metrics to measure the naturalness and correctness of the generated gesture movements, namely Fréchet Gesture Distance (FGD), Beat Consistency Score (BC), and Diversity. More description on these metrics can be found in the Appendix.

## Evaluation Results

**Quantitative Results.** We first compare C2G2 with existing baselines on the above 3 metrics. For the real-length skeleton generation obtained from C2G2-*rl*, we use the same FGD model in HA2G (Liu et al. 2022) but normalize the final results back to unit direction vectors for the fair comparison. All the comparison results are shown in Table 1. From the table, we observe that VQ-VAE reconstruction achieves comparable results with the ground-truth ones, which shows the excellent reconstruction capability of the proposed temporal-aware VQ-VAE.

For the metric FGD, both C2G2 and C2G2-*rl* achieve significant improvements on the two datasets. Specifically, C2G2-*rl* is consistently the winner among all the baselines, achieving 0.854 and 1.505 lower values than the best baseline DiffGesture. C2G2 is the runner-up, which yields better results than all existing baselines but inferior results than C2G2-*rl*. These results demonstrate that our C2G2 can generate more realistic gestures as FGD mainly reflects the distance of the generated distribution with the real one.

For the metric diversity, although C2G2-*rl* obtains the best result on TED Expressive, we also note that it fails on TED Gesture. We suspect the reason is because the gesture space of TED Gesture is not that diversified and C2G2-*rl* is over-fitted, as indicated by its smallest FGD value, and thus constrains the generation diversity. However, such an inferiority disappears on TED Expressive containing more complicated figure movements. As can be seen, C2G2-*rl* is a clear winner among all the baselines for diversity on TED Expressive.

Finally, for the metric BC, C2G2-*rl* and C2G2 generally achieve competitive results with the best baseline DiffGesture. Future studies will put the focus on more powerful audio encoder to further boost the BC performance.

**Qualitative Results.** In this section, we visualize the generated gestures from different methods for the qualitative comparison. Considering that HA2G (Liu et al. 2022) and DiffGesture (Zhu et al. 2023) outperform the other baselines as presented in their paper, we mainly compare C2G2 with these two methods. The visualization results are illustrated in Figure 4. As can be seen, HA2G generates wired and slow gesture movements without proper matching with the input audio. This is because HA2G may suffer from the model collapse issue during training. DiffGesture generally achieves

	Metric	Ground-truth	HA2G	Diffgesture	C2G2
Short Clips	NAL	3.438	3.275	3.144	<b>3.506</b>
	SMTH	3.325	3.144	3.144	<b>3.681</b>
	SYN	<b>3.494</b>	3.331	3.294	3.350
Long Clips	NAL	2.916	3.056	2.741	<b>3.394</b>
	SMTH	2.894	2.992	2.870	<b>3.384</b>
	SYN	<b>3.411</b>	3.028	3.247	3.304
Middle Clips	NAL	<b>4.009</b>	3.275	3.456	3.903
	SMTH	3.894	2.759	2.850	<b>4.072</b>
	SYN	<b>4.128</b>	3.175	3.734	3.881
Average	NAL	3.469	3.219	3.163	<b>3.619</b>
	SMTH	3.363	3.003	3.025	<b>3.738</b>
	SYN	<b>3.647</b>	3.216	3.413	3.522

Table 2: User study. MOS scores for the naturalness (NAL), smoothness (SMTH) and synchrony (SYN) of the generated gesture sequences. Short and long clips are for successive generation, and middle clips are for in-betweening generation. We compare C2G2 with HA2G and DiffGesture.

good continuity, however, it is easily stuck into one gesture for several frames, leading to a weak correlation with the input audios. Among the three methods, C2G2 can ensure both the temporal smoothness and semantic correlation with the input audios.

**User Study.** We further conduct a subjective user study to measure the naturalness, smoothness and synchrony of the generated gesture sequences for different methods. Specifically, we randomly sample 20 clips from TED Expressive, including 10 short clips (each with  $\sim 2$ s), 5 long clips (each with  $\sim 60$ s) and 5 middle-length clips (each with  $\sim 10$ s). The short and long clips are used to evaluate the short-term and long-term successive generation quality, while the middle-length clips are used for the evaluation of the in-betweening generation. Specifically, for each middle-length clip, the first 4 frames and the last  $\sim 25$  frames are pre-given, and the intermediate frames are to be generated. We invite 8 volunteers to give the score for the generated gesture sequences from 3 perspectives: naturalness, smoothness and synchrony. The ratings are from 1 to 5 with 5 marking the highest quality. The detailed scoring rules are presented in the Appendix. Mean Opinion Score (MOS) is then calculated based on the evaluation results and is shown in Table 2.

From Table 2, we can see that C2G2 consistently ensures the better naturalness, synchrony and smoothness compared with DiffGesture and HA2G in average. More specifically, all the methods generally perform better in short clips than in long clips. This is reasonable as long sequences indicate more complex and diversified gestures included. It is surprising that our generated gestures have even higher naturalness and smoothness than the Ground-Truth ones, which demonstrates the superiority of C2G2 in the successive generation scenario. Moreover, C2G2 achieves more significant improvements in middle clips generation, where the repainting strategy is applied, especially on smoothness. This verifies that C2G2 can also generate high-quality gestures in the in-betweening generation scenario, while existing methods usually have an obvious gap in the transition part between the generated and real frames. All these results prove that

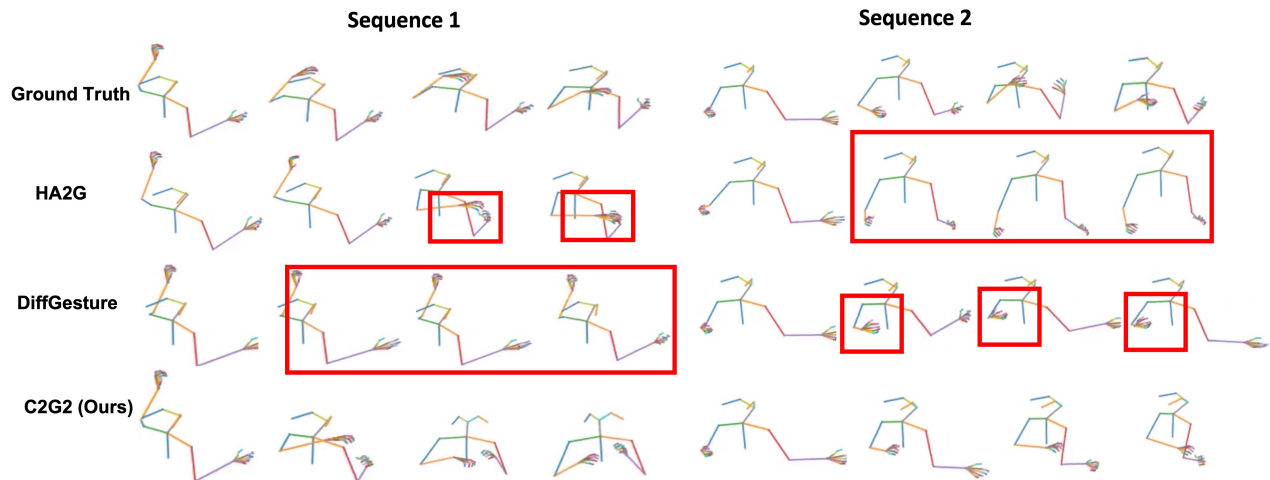


Figure 4: The visualization results of generated gesture sequence from C2G2 and previous methods (Liu et al. 2022; Zhu et al. 2023). Two sequences, each with four continuous frames, are selected. We highlight the slowly changed or nearly frozen frames in the generated results with red rectangles.

Methods	Ted Gesture		Ted Expressive	
	FGD↓	Diversity↑	FGD↓	Diversity↑
Ground Truth	0.000	108.525	0.000	178.827
$V_{w/o\_enc\_trans}$	3.959	98.707	4.939	170.039
$V_{w/o\_dec\_trans}$	10.098	95.335	23.292	158.320
Full VQ-VAE	<b>0.109</b>	<b>107.450</b>	<b>0.402</b>	<b>179.743</b>

Table 3: Ablation study results of encoder-decoder structure w/o temporal transformer module.

C2G2 is a promising co-speech gesture generation model.

## Ablation Study

**Ablation Study on VQ-VAE Structure.** To verify the temporal coherence enhancement brought by the temporal-aware VQ-VAE, we propose to compare with two more variants. The first variant is a VQ-VAE without transformer module in the encoder, and the second one is a VQ-VAE without transformer module in the decoder. We compare the two variants with the full VQ-VAE with respect to FGD and diversity on both TED Gesture and Expressive datasets. The comparison results are shown in Table 3. From Table 3, we can easily observe that transformer layers are both necessary in encoder and decoder to improve the quantization performance by capturing temporal information.

**Ablation Study on Quantizer of VQ-VAE.** Compared with TED Gesture, TED Expressive contains more complicated information due to fine-grained finger keypoints (8 basic skeleton keypoints and 15 keypoints per hand). Thus, a more powerful quantizer is crucial for the quantization of the gesture sequences in TED Expressive. We conduct ablation studies with respect to EMA and Reset strategies on TED Expressive. We mainly compare with the quantizer (1) without both EMA and Reset strategy, (2) without EMA strategy, and (3) without Reset Strategy. The results are shown

Method	EMA	Reset	FGD↓	Diversity↑
Ground Truth			0	178.827
Quantizer			21.495	151.653
Quantizer	✓		0.670	180.829
Quantizer		✓	0.522	<b>180.876</b>
Quantizer	✓	✓	<b>0.402</b>	179.743

Table 4: Ablation study results of different quantizer w/o EMA or Reset strategies on TED Expressive.

in Table 4. As can be seen, quantizer with both EMA code-book updating and reset of inactive codes can achieve good reconstruction performance with the lowest FGD and competitive diversity.

## Conclusion

In this paper, we propose a novel latent diffusion based co-speech generation framework named **C2G2** that enables two different gesture controlling. To better enhance the temporal consistency, we leverage a two-stage latent diffusion model composed of a temporal-aware VQ-VAE and transformer based diffusion noise predictor. Moreover, considering more practical scenarios, we allow speaker’s real-length conditioning and movement editing through SRD module and repainting sampling strategy. Extensive experimental studies including both quantitative and qualitative evaluations demonstrate the effectiveness of our C2G2 compared with several state-of-the-art baselines. We also remark some limitations and future working directions for our work. Firstly, the pre-trained models may contain bias towards a single language as it is trained on an English-based dataset. Multi-linguistic dataset collection is a worthy direction for the community for more general co-speech gesture generation. Moreover, our model composes of two-stage training as well

as one more step of speaker decoder finetuning, thus may result in unstable generation quality due to the stage-level error propagation.

## References

- Ahuja, C.; Lee, D. W.; Ishii, R.; and Morency, L.-P. 2020a. No gestures left behind: Learning relationships between spoken language and freeform gestures. In *Findings of the Association for Computational Linguistics: EMNLP 2020*, 1884–1895.
- Ahuja, C.; Lee, D. W.; Nakano, Y. I.; and Morency, L.-P. 2020b. Style transfer for co-speech gesture animation: A multi-speaker conditional-mixture approach. In *Computer Vision–ECCV 2020: 16th European Conference, Glasgow, UK, August 23–28, 2020, Proceedings, Part XVIII 16*, 248–265. Springer.
- Ahuja, C.; and Morency, L.-P. 2019. Language2pose: Natural language grounded pose forecasting. In *2019 International Conference on 3D Vision (3DV)*, 719–728. IEEE.
- Alexanderson, S.; Henter, G. E.; Kucherenko, T.; and Beskow, J. 2020. Style-controllable speech-driven gesture synthesis using normalising flows. In *Computer Graphics Forum*, volume 39, 487–496. Wiley Online Library.
- Ao, T.; Gao, Q.; Lou, Y.; Chen, B.; and Liu, L. 2022. Rhythmic gesticulator: Rhythm-aware co-speech gesture synthesis with hierarchical neural embeddings. *ACM Transactions on Graphics (TOG)*, 41(6): 1–19.
- Ao, T.; Zhang, Z.; and Liu, L. 2023. GestureDiffuCLIP: Gesture diffusion model with CLIP latents. *arXiv preprint arXiv:2303.14613*.
- Bhattacharya, U.; Rewkowski, N.; Banerjee, A.; Guhan, P.; Bera, A.; and Manocha, D. 2021. Text2gestures: A transformer-based network for generating emotive body gestures for virtual agents. In *2021 IEEE virtual reality and 3D user interfaces (VR)*, 1–10. IEEE.
- Cao, Z.; Simon, T.; Wei, S.-E.; and Sheikh, Y. 2017. Realtime multi-person 2d pose estimation using part affinity fields. In *Proceedings of the IEEE conference on computer vision and pattern recognition*, 7291–7299.
- Cassell, J.; Pelachaud, C.; Badler, N.; Steedman, M.; Achorn, B.; Becket, T.; Douville, B.; Prevost, S.; and Stone, M. 1994. Animated conversation: rule-based generation of facial expression, gesture & spoken intonation for multiple conversational agents. In *Proceedings of the 21st annual conference on Computer graphics and interactive techniques*, 413–420.
- Choutas, V.; Pavlakos, G.; Bolkart, T.; Tzionas, D.; and Black, M. J. 2020a. Monocular Expressive Body Regression through Body-Driven Attention. In *European Conference on Computer Vision (ECCV)*, 20–40.
- Choutas, V.; Pavlakos, G.; Bolkart, T.; Tzionas, D.; and Black, M. J. 2020b. Monocular expressive body regression through body-driven attention. In *Computer Vision–ECCV 2020: 16th European Conference, Glasgow, UK, August 23–28, 2020, Proceedings, Part X 16*, 20–40. Springer.
- Dhariwal, P.; and Nichol, A. 2021. Diffusion models beat gans on image synthesis. *Advances in neural information processing systems*, 34: 8780–8794.
- Ellis, D. P. 2007. Beat tracking by dynamic programming. *Journal of New Music Research*, 36(1): 51–60.
- Esser, P.; Rombach, R.; and Ommer, B. 2020. Taming Transformers for High-Resolution Image Synthesis. *arXiv:2012.09841*.
- Ferstl, Y.; Neff, M.; and McDonnell, R. 2020. Adversarial gesture generation with realistic gesture phasing. *Computers & Graphics*, 89: 117–130.
- Ginosar, S.; Bar, A.; Kohavi, G.; Chan, C.; Owens, A.; and Malik, J. 2019a. Learning Individual Styles of Conversational Gesture. In *Computer Vision and Pattern Recognition (CVPR)*. IEEE.
- Ginosar, S.; Bar, A.; Kohavi, G.; Chan, C.; Owens, A.; and Malik, J. 2019b. Learning individual styles of conversational gesture. In *Proceedings of the IEEE/CVF Conference on Computer Vision and Pattern Recognition*, 3497–3506.
- Goldin-Meadow, S. 2005. *Hearing gesture: How our hands help us think*. Harvard University Press.
- Goldin-Meadow, S.; and McNeill, D. 1999. *The role of gesture and mimetic representation in making language the province of speech*. na.
- Hasegawa, D.; Kaneko, N.; Shirakawa, S.; Sakuta, H.; and Sumi, K. 2018. Evaluation of speech-to-gesture generation using bi-directional LSTM network. In *Proceedings of the 18th International Conference on Intelligent Virtual Agents*, 79–86.
- Heusel, M.; Ramsauer, H.; Unterthiner, T.; Nessler, B.; and Hochreiter, S. 2017. Gans trained by a two time-scale update rule converge to a local nash equilibrium. *Advances in neural information processing systems*, 30.
- Ho, J.; Jain, A.; and Abbeel, P. 2020. Denoising diffusion probabilistic models. *Advances in neural information processing systems*, 33: 6840–6851.
- Huang, C.-M.; and Mutlu, B. 2012. Robot behavior toolkit: generating effective social behaviors for robots. In *Proceedings of the seventh annual ACM/IEEE international conference on Human-Robot Interaction*, 25–32.
- Huang, R.; Huang, J.; Yang, D.; Ren, Y.; Liu, L.; Li, M.; Ye, Z.; Liu, J.; Yin, X.; and Zhao, Z. 2023. Make-an-audio: Text-to-audio generation with prompt-enhanced diffusion models. *arXiv preprint arXiv:2301.12661*.
- Ishi, C. T.; Machiyashiki, D.; Mikata, R.; and Ishiguro, H. 2018. A speech-driven hand gesture generation method and evaluation in android robots. *IEEE Robotics and Automation Letters*, 3(4): 3757–3764.
- Kong, Z.; Ping, W.; Huang, J.; Zhao, K.; and Catanzaro, B. 2020. Diffwave: A versatile diffusion model for audio synthesis. *arXiv preprint arXiv:2009.09761*.
- Kucherenko, T.; Hasegawa, D.; Henter, G. E.; Kaneko, N.; and Kjellström, H. 2019. Analyzing input and output representations for speech-driven gesture generation. In *Proceedings of the 19th ACM International Conference on Intelligent Virtual Agents*, 97–104.



- Lee, H.-Y.; Yang, X.; Liu, M.-Y.; Wang, T.-C.; Lu, Y.-D.; Yang, M.-H.; and Kautz, J. 2019. Dancing to music. *Advances in neural information processing systems*, 32.
- Li, B.; Zhao, Y.; Zhelun, S.; and Sheng, L. 2022. Danceformer: Music conditioned 3d dance generation with parametric motion transformer. In *Proceedings of the AAAI Conference on Artificial Intelligence*, volume 36, 1272–1279.
- Li, J.; Kang, D.; Pei, W.; Zhe, X.; Zhang, Y.; He, Z.; and Bao, L. 2021a. Audio2gestures: Generating diverse gestures from speech audio with conditional variational autoencoders. In *Proceedings of the IEEE/CVF International Conference on Computer Vision*, 11293–11302.
- Li, R.; Yang, S.; Ross, D. A.; and Kanazawa, A. 2021b. Ai choreographer: Music conditioned 3d dance generation with aist++. In *Proceedings of the IEEE/CVF International Conference on Computer Vision*, 13401–13412.
- Liu, X.; Wu, Q.; Zhou, H.; Xu, Y.; Qian, R.; Lin, X.; Zhou, X.; Wu, W.; Dai, B.; and Zhou, B. 2022. Learning hierarchical cross-modal association for co-speech gesture generation. In *Proceedings of the IEEE/CVF Conference on Computer Vision and Pattern Recognition*, 10462–10472.
- Lu, S.; Yoon, Y.; and Feng, A. 2023. Co-Speech Gesture Synthesis using Discrete Gesture Token Learning. *arXiv preprint arXiv:2303.12822*.
- Lugmayr, A.; Danelljan, M.; Romero, A.; Yu, F.; Timofte, R.; and Van Gool, L. 2022. Repaint: Inpainting using denoising diffusion probabilistic models. In *Proceedings of the IEEE/CVF Conference on Computer Vision and Pattern Recognition*, 11461–11471.
- Luo, S.; and Hu, W. 2021. Diffusion probabilistic models for 3d point cloud generation. In *Proceedings of the IEEE/CVF Conference on Computer Vision and Pattern Recognition*, 2837–2845.
- Marsella, S.; Xu, Y.; Lhommet, M.; Feng, A.; Scherer, S.; and Shapiro, A. 2013. Virtual character performance from speech. In *Proceedings of the 12th ACM SIGGRAPH/Eurographics symposium on computer animation*, 25–35.
- Nyatsanga, S.; Kucherenko, T.; Ahuja, C.; Henter, G. E.; and Neff, M. 2023. A Comprehensive Review of Data-Driven Co-Speech Gesture Generation. In *Computer Graphics Forum*, volume 42, 569–596. Wiley Online Library.
- Pavlakos, G.; Choutas, V.; Ghorbani, N.; Bolkart, T.; Osman, A. A. A.; Tzionas, D.; and Black, M. J. 2019. Expressive Body Capture: 3D Hands, Face, and Body from a Single Image. In *Proceedings IEEE Conf. on Computer Vision and Pattern Recognition (CVPR)*, 10975–10985.
- Qi, X.; Liu, C.; Li, L.; Hou, J.; Xin, H.; and Yu, X. 2023. EmotionGesture: Audio-Driven Diverse Emotional Co-Speech 3D Gesture Generation. *arXiv preprint arXiv:2305.18891*.
- Razavi, A.; Van den Oord, A.; and Vinyals, O. 2019. Generating diverse high-fidelity images with vq-vae-2. *Advances in neural information processing systems*, 32.
- Rombach, R.; Blattmann, A.; Lorenz, D.; Esser, P.; and Ommer, B. 2022. High-resolution image synthesis with latent diffusion models. In *Proceedings of the IEEE/CVF conference on computer vision and pattern recognition*, 10684–10695.
- Van Den Oord, A.; Vinyals, O.; et al. 2017. Neural discrete representation learning. *Advances in neural information processing systems*, 30.
- Yang, S.; Wu, Z.; Li, M.; Zhang, Z.; Hao, L.; Bao, W.; Cheng, M.; and Xiao, L. 2023. DiffuseStyleGesture: Stylized Audio-Driven Co-Speech Gesture Generation with Diffusion Models. *arXiv preprint arXiv:2305.04919*.
- Yang, Y.; Yang, J.; and Hodgins, J. 2020. Statistics-based motion synthesis for social conversations. In *Computer Graphics Forum*, volume 39, 201–212. Wiley Online Library.
- Ye, Z.; Jia, J.; Wu, H.; Huang, S.; Sun, S.; and Xing, J. 2023. Salient Co-Speech Gesture Synthesizing with Discrete Motion Representation. In *ICASSP 2023-2023 IEEE International Conference on Acoustics, Speech and Signal Processing (ICASSP)*, 1–5. IEEE.
- Yi, H.; Liang, H.; Liu, Y.; Cao, Q.; Wen, Y.; Bolkart, T.; Tao, D.; and Black, M. J. 2023. Generating holistic 3d human motion from speech. In *Proceedings of the IEEE/CVF Conference on Computer Vision and Pattern Recognition*, 469–480.
- Yoon, Y.; Cha, B.; Lee, J.-H.; Jang, M.; Lee, J.; Kim, J.; and Lee, G. 2020. Speech gesture generation from the trimodal context of text, audio, and speaker identity. *ACM Transactions on Graphics (TOG)*, 39(6): 1–16.
- Yoon, Y.; Ko, W.-R.; Jang, M.; Lee, J.; Kim, J.; and Lee, G. 2019. Robots learn social skills: End-to-end learning of co-speech gesture generation for humanoid robots. In *2019 International Conference on Robotics and Automation (ICRA)*, 4303–4309. IEEE.
- Zhang, J.; Zhang, Y.; Cun, X.; Huang, S.; Zhang, Y.; Zhao, H.; Lu, H.; and Shen, X. 2023. T2M-GPT: Generating Human Motion from Textual Descriptions with Discrete Representations. In *Proceedings of the IEEE/CVF Conference on Computer Vision and Pattern Recognition (CVPR)*.
- Zhu, L.; Liu, X.; Liu, X.; Qian, R.; Liu, Z.; and Yu, L. 2023. Taming Diffusion Models for Audio-Driven Co-Speech Gesture Generation. In *Proceedings of the IEEE/CVF Conference on Computer Vision and Pattern Recognition*, 10544–10553.

Block	Shape	Operation
<b>VQ-VAE Encoder</b>		
input	34*126	
LIN(126,128)	34*128	Linear,LN,LeakyReLU
ResLIN(128,128)	34*128	Linear,LN,Linear,LN
ResLIN(128,256)	34*256	Linear,LN,Linear,LN
ResLIN(256,512)	34*512	Linear,LN,Linear,LN
ResLIN(512,256)	34*256	Linear,LN,Linear,LN
ResLIN(256,128)	34*128	Linear,LN,Linear,LN
LIN(128,128)	34*128	Linear,LN,LeakyReLU
Position-Encoder	34*128	Positional Embedding
Trans-Block *4	34*128	Self-attention,FFN
LIN(128,128)	34*128	Linear,LN,LeakyReLU
Quant-Conv(128,128)	34*128	Conv1d
<b>Audio Encoder</b>		
Convolution layer1	16*7891	Conv1d,BN,LeakyReLU
Convolution layer2	32*1313	Conv1d,BN,LeakyReLU
Convolution layer3	64*217	Conv1d,BN,LeakyReLU
Convolution layer4	32*34	Conv1d
<b>Latent Diffusion Model</b>		
LIN-In	34*256	Linear,LN,LeakyReLU
Trans-Block*8	34*256	self-attention, FFN
LIN-Out-1	34*128	Linear,LN,LeakyReLU
LINr-Out-2	34*128	Linear

Table 5: Detailed architecture of C2G2.

## Appendix

In the supplementary material, we 1) provide more model details of C2G2, 2) give the detailed description of evaluation metrics 3) show more experimental details on C2G2.

### Model Details

#### C2G2 Model Architecture

We provide the detailed model architecture of C2G2 as shown in Table 5. We only give the description of the encoder in temporal-aware VQVAE. The decoder has symmetric structure with encoder but with different number of Trans-Blocks (4 in encoder, 2 in decoder).

#### In-betweening Editing Details

In-betweening generation allows to generate gestures between pre-condition frames and post-condition frames. It can be further used to add/replace short movements to any position of a long sequence. Specifically, in the user study, i.e., the middle clip (34 frames in total) generation, repainting strategy applies in the generation of the last clip where last 10 frames are post-condition frames. However, only 6 frames before the post-condition frames are used as the transition part and are generated using repainting strategy, while the former frames are still sampled from noise.

Methods	Shape		TED Expressive	
	Size	Channel	FGD ↓	Diversity ↑
Ground-Truth			0	178.827
VQ-VAE	512	64	0.854	178.245
VQ-VAE	512	128	0.849	178.888
VQ-VAE	512	256	0.588	179.366
VQ-VAE	1024	64	0.560	<b>180.261</b>
VQ-VAE	1024	128	<b>0.402</b>	179.743
VQ-VAE	1024	256	0.526	178.918

Table 6: Ablation study results of different codebook shapes in terms of codebook size and code channels.

## Evaluation Metrics

In the evaluation, we adopt three different metrics to measure the naturalness and correctness of the generated gesture sequences.

**Frechet Gesture Distance (FGD).** Similar as Frechet Inception Distance (FID) (Heusel et al. 2017), we use an autoencoder pretrained on both datasets to compute the distance between the generated gesture sequences and the real ones in the latent feature space. FGD is the metric best describing the synthesis quality of the generated sequences.

**Beat Consistency Score (BC).** To measure the correlation of generated gesture sequences and the corresponding audio sequences, we use Beat Consistency (BC) (Li et al. 2022, 2021b). To obtain BC, we need to first calculate the mean absolute angle change (Liu et al. 2022), followed by the angle change rate. Motion beats are then estimated by using such a change of included angle between bones. Following (Ellis 2007), we detect the audio beats by onset strength (Li et al. 2022). Finally, we calculate the average distance between the audio beat and its nearest motion beat to serve as Beat Consistency Score.

**Diversity.** The metric measures the variation of generated gestures compared with corresponding inputs (Lee et al. 2019). Specifically, it is calculated as the mean distance of a set of generated sequences and its randomly shuffled variant in the latent feature space that is described in FGD. In practice, we randomly select 500 different gesture sequences and then calculate the average feature distance accordingly.

## More Experimental Results

### Ablation Study on Codebook Shape

To analyze the effect of the codebook shape on the VQ-VAE performance, we conduct experiments on various settings with different codebook size and code channels (dimensionality). We test 6 settings in total with different codebook sizes and code channels, where the results are show in Table 6. The result reveal that, in the setting of (1024, 128), the VQ-VAE model achieves the best performance as reported in the main paper. We do not consider more channels as this leads to the difficulty and high cost of diffusion training, which hinders the practical usage.

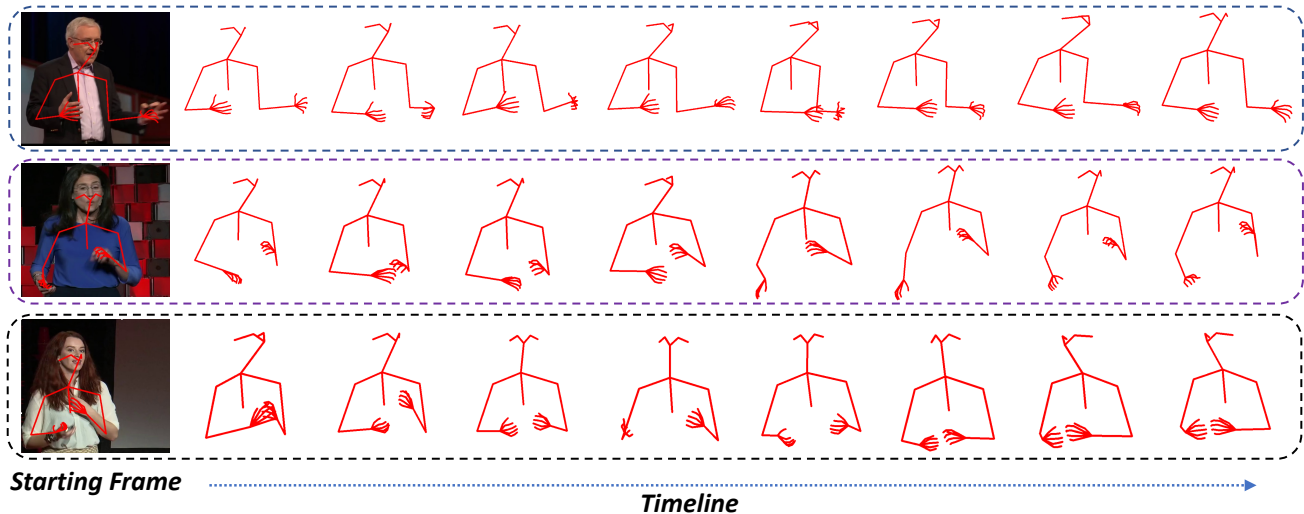


Figure 5: Visualization of speaker conditional generation.

Methods	Shape		TED Expressive	
	Size	Channel	FGD ↓	Rec-loss ↓
Ground Truth			0.000	0.000
VQ-VAE <sub>rl</sub>	1024	64	281.65	0.021
VQ-VAE <sub>rl</sub>	1024	128	283.40	0.019
VQ-VAE <sub>rl</sub>	1024	256	280.01	0.021
VQ-VAE <sub>rl</sub>	2048	128	282.22	0.019
VQ-VAE <sub>rl</sub>	2048	256	283.66	0.019
VQ-VAE <sub>ours</sub>	1024	128	<b>0.341</b>	<b>0.005</b>

Table 7: Results of VQ-VAE trained by real-length vectors on various codebook settings.

### Real-length Input Training Pipeline

In the paper, the VQ-VAE is trained using gesture sequences represented by unit vectors and then the speaker information is then introduced through a specifically designed speaker related decoder. The reason of not directly using real-length vectors is because this will lead to unstable training (not converging) and thus jeopardize the generated results. To verify this, we conduct experiments of directly reconstructing real-length gestures by VQ-VAE without using the SRD. As shown in table 7, VQ-VAE trained with the real-length vectors faces serious mode collapse issue and poor reconstruction results on various settings of codebook size and code channel.

### Subjective Evaluation Protocol

For the user study, we design a detailed scoring protocol for the subjective evaluation. Rating score is from 1 to 5 with 1 as the worst and 5 as the best. We give the detailed descriptions for score 1, 3 and 5.

#### Naturalness:

- 1 point - generated gesture sequence is totally unnatural, and may contain serious frozen, distortion and shaking movements.

- 3 point - generated gesture sequence is partially natural, part of the poses may include generated traces of unreasonable movements or sight frozen.
- 5 point - generated gesture sequence follows the usual movement habits and margins of real humans without noticeable issues.

#### Smoothness:

- 1 point - result has observe inconsistency across temporal sequence and body parts. Rapid changes usually happen between frames.
- 3 point - body skeleton is mainly temporal consistent with satisfied smoothness. Inconsistency may occur in hands.
- 5 point - overall result has strong temporal consistency and is smooth both in body and hands.

#### Synchrony:

- 1 point - generated gesture sequence has no related alignment for the speech content and beat.
- 3 point - generated gesture sequence is synchronized with the input speech in several parts, and correlation could be observed.
- 5 point - generated gesture sequence is highly aligned with the accompanied speech, and no unrelated gesture is observed in the whole sequence.

### Visualization Results

We provide more visualization results in this section. In figure 5, we show the generated results of 3 different speakers. In figure 6, we show the smooth generation results of the in-betweening case. More video samples can be found in our demo page <https://c2g2-gesture.github.io/c2-gesture/>.

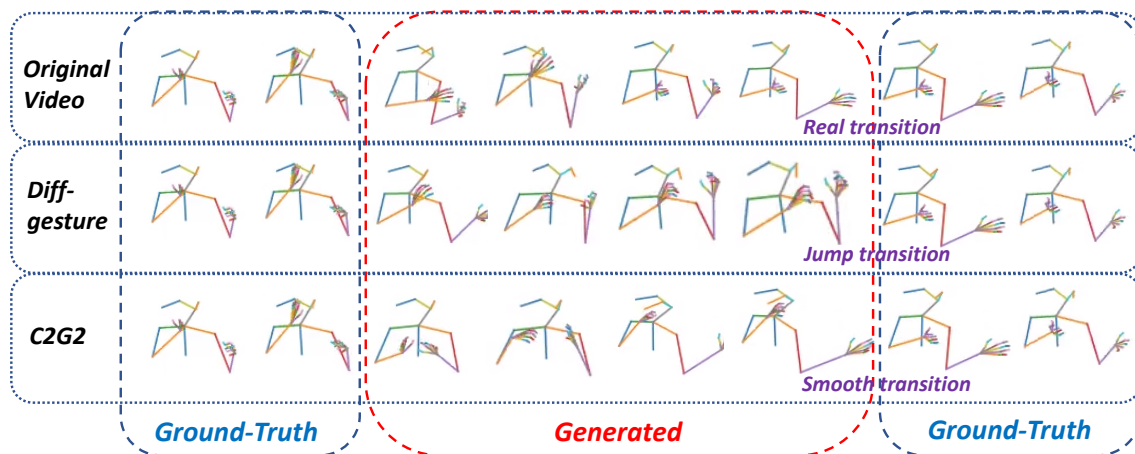


Figure 6: Visualization of in-betweening generation.